Original Article

Three dimensional reconstruction and measurement of underwater spent fuel assemblies

Jianping Zhao [a, b], Shengbo He [a], Li Yang [a], Chang Feng [a, b], Guoqiang Wu [a], Gen Cai [a, b, *]

[a] *Institute of Optics and Electronics, Chinese Academy of Sciences, Chengdu, 610209, China*
[b] *University of Chinese Academy of Sciences, Beijing, 100049, China*

ABSTRACT

It is an important work to measure the dimensions of underwater spent fuel assemblies in the nuclear power industry during the overhaul, to judging whether the spent fuel assemblies can continue to be used. In this paper, a three dimensional reconstruction method for underwater spent fuel assemblies of nuclear reactor based on linear structured light is proposed, and the topography and size measurement was carried out based on the reconstructed 3D model. Multiple linear structured light sensors are used to obtain contour size data, and the shape data of the whole spent fuel assembly can be collected by one-dimensional scanning motion. In this paper, we also presented a corrected model to correct the measurement error introduced by lead-glass and water is corrected. Then, we set up an underwater measurement system for spent fuel assembly based on this method. Finally, an underwater measurement experiment is carried out to verify the 3D reconstruction ability and measurement ability of the system, and the measurement error is less than ±0.05 mm.

1. Introduction

Nuclear power is an important option for many countries as a stable and clean source of energy. Fuel assembly converts nuclear energy into heat energy and is an important part of nuclear reaction. After the fuel assembly runs in the high pressure, high temperature, and underwater corrosion environment of the reactor, the fuel assembly may appear expansion, bending, twisting and other phenomena. There is a risk of damage and leakage if an abnormal fuel assembly is re-used in the reactor. Therefore, it is an important work to measure the dimensions of underwater spent fuel assemblies in the nuclear power industry during the overhaul, to judging whether the spent fuel assemblies can continue to be used [1].

Due to the high radiation dose of the spent fuel assembly, the inspection of the fuel assembly is usually carried out in the spent fuel pool or hot cell. Non-contact measurement and contact measurement are the main measurement methods to measure the dimensions of spent fuel assemblies. Contact measurement mainly adopts linear displacement sensor, while non-contact measurement adopts vision sensors. The two measurement methods have

their own advantages and disadvantages. The contact measurement method has strong irradiation resistance, but the measurement points are sparse. Furthermore, the contact measurement method is time-consuming and has a risk of scratching the fuel rods. Non-contact measurement has high measurement accuracy and dense measurement points, but it has poor irradiation resistance and many challenges in underwater applications. Siguero et al. developed a spent fuel assemblies deformation detection system adopted underwater LVDT probes, with a measurement error of ±0.2 mm [2]. Sasaki et al. adopted linear displacement sensor to measure the dimensions of the fuel assemblies from sodium-cooled fast reactor in hot cell with a measurement error of ±0.1 mm [3]. But, the above two sets of equipment are time-consuming and the measurement points were spaced widely. Zavyalov P.S et al. proposed a sodium-cooled fast reactor's fuel assemblies measurement system based on point structured light in hot cell, and the measurement error was less than ±0.3 mm in the direction of measurement, but there are very few measurement points [4]. Ahlberg and Joakim proposed a spent fuel assembly measurement system based on four cameras and provided a 3D model after image capture [1]. JAIWAN CHO et al. at the Korea Atomic Energy Research Institute used structured light measurement to check the deformation of fuel rods. The measurement resolution was up to 50um at a measurement distance of 440 mm,

but the measurement coverage of the system was limited to 20mm × 20 mm [5]. Congzheng Wang et al. realized the spent fuel assemblies inspection base on underwater camera array measurement system, and the measurement error was less than ±0.5 mm [6]. In addition, Institute of Optics and Electronics of Chinese Academy of Sciences and China Institute of Atomic Energy jointly developed a three-dimensional reconstruction and measurement system of fuel assemblies for Sodium-cooled fast reactor using linear structured light, and successfully applied it in the hot cell with the measurement error less than ±0.05 mm [7].

Since the risk of fuel assembly damage, low measurement efficiency, sparse measurement points and other factors, contact measurement has been rarely used in intense radiation underwater environment. Visual measurement methods such as linear structured light and binocular measurement have the advantages of non-contact and dense collection points, which are increasingly applied in the field of nuclear industry. In this paper, an underwater 3D reconstruction method of fuel assembly is proposed. The complete surface profile of fuel assembly is captured by multiple linear structured light (LSL) sensors, combined with high-precision axial scanning. An underwater measurement system for spent fuel assembly was designed and manufactured based on this method.

2. Method

2.1. System configuration

The underwater LSL measurement system for spent fuel assembly is composed of underwater LSL measuring body and control cabinet. The underwater measuring body and the control cabinet are connected by underwater cables. The operator remotely controls the underwater measuring body at the main control computer, at the same time, the motion process of the device is monitored by the camera mounted on the linear structured light measurement module.

The underwater LSL measuring body includes the driving module, the vertical frame, the lifting platform, the underwater LSL measurement modules, the encoder module, the counterweight module, the clamping module, the base so on. The base and vertical frame are the main frame of the measuring system, which are used to install and fix the other parts. The clamping module is installed on the base and is used to clamp the spent fuel assembly. The underwater LSL measurement modules are installed on the lifting platform, and the driving module drives the lifting platform to move. The driving module is composed of a driving motor, a reducer and a chain drive mechanism. One end of the chain is connected to the lifting platform and the other end is connected to the counterweight module. The counterweight module is used to offset the weight of the lifting platform and measuring module. The encoder module is used to trigger the four underwater LSL measurement modules to obtain point cloud data and calculate height value at the same time.

During inspection, the lifting platform first drops to the lower limit, and then starts to move upward from the lower limit. When the motion reaches zero, the encoder starts to trigger the LSL measurement module to collect the surface contour data of the underwater spent fuel assembly. The data collected by the four LSL measurement modules are fused into one by the data processing system and reconstructed the three-dimensional model [7], and the measurement operation is carried out based on the point cloud data.

The control cabinet is composed of PLC, main control computer, display, main power source and other components. The PLC is used to adopt the signal of each limit switch and send the control signal to drive motor. The main control computer's is a control station

with operating software and graphical user interfaces, its function is to control underwater LSL measuring body and process the contour data (see Fig. 1).

2.2. Underwater LSL measurement module

The underwater LSL measurement module is the most important part of the system, which is used to obtain the spent fuel assembly profile. The system consists of four underwater LSL measurement modules, which are arranged on the lifting platform to cover the complete section profile of the spent fuel assembly, as shown in Fig. 2.

The linear structured light sensor consists of a camera and a laser, which are arranged in a certain position relationship (see Fig. 3). Camera and laser are electronic devices with limited radiation resistance and not waterproof. The spent fuel assemblies, while not in working condition, still emit large amounts of gamma rays which will cause electronic device failure [8–10] and make the image sensor appear irradiation noise [11,12], and then result in lower measurement accuracy and shorter lifetime of the system. On the other hand, LSL sensors are not waterproof and need to be protected by sealed glass when used underwater. In this paper, a thick lead-glass is installed in front of the underwater LSL measurement module, and the lead-glass plays the role of gamma rays shield [13,14] and waterproof. In order to further improve the radiation resistance of the LSL sensor, the radiation resistant glass is designed as a right-angle reflection prism. In addition, the thickest tungsten alloy is installed in the direction facing the assembly, followed by the thickest on the sides and the thinnest on the back. The outer part of the underwater LSL measurement module is stainless steel sealing chamber and sealing cover, used for waterproof.
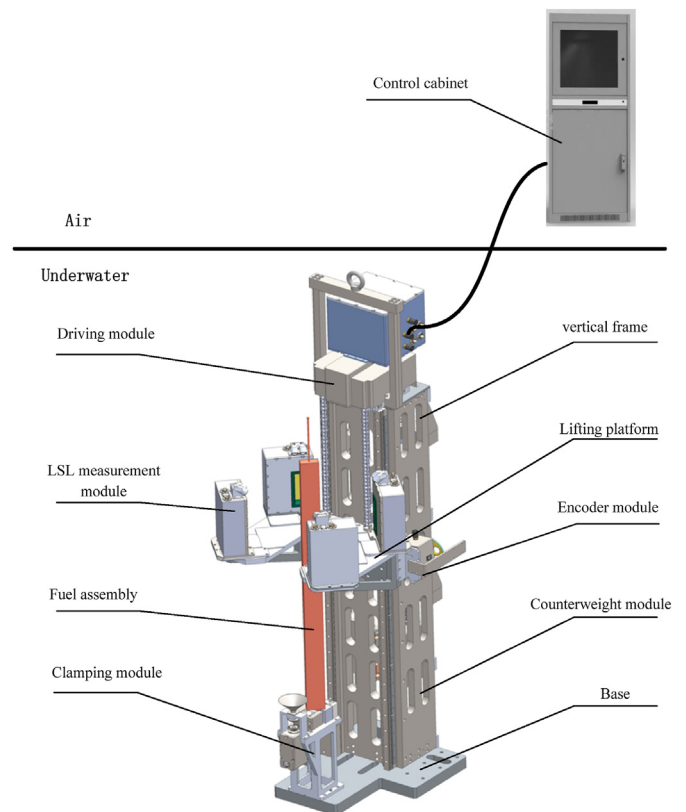

Fig. 1. System configuration of the underwater LSL measurement system for spent fuel assembly.
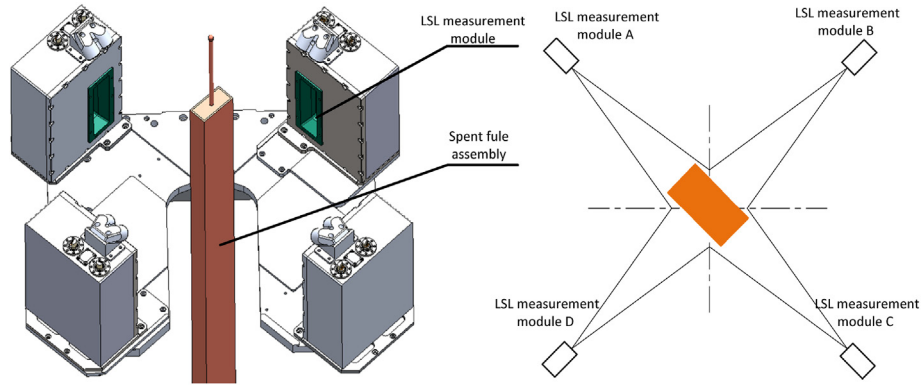
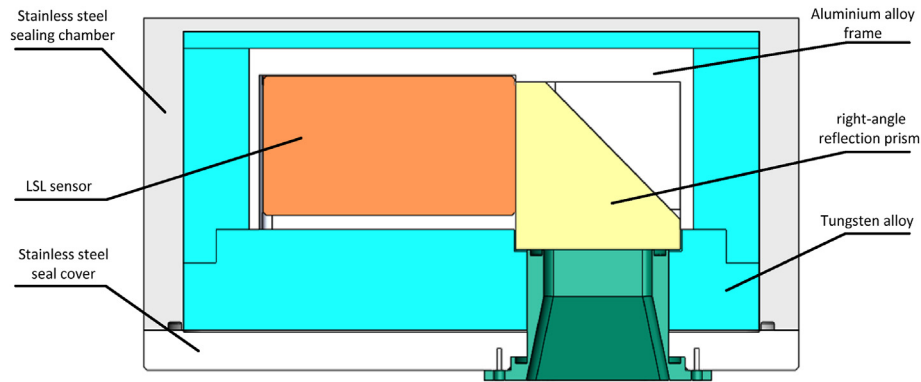**Fig. 2.** Installation position of underwater LSL measurement module.

Fig. 3. Section view of the underwater LSL measurement module.

The right-angle reflection prism made of lead-glass is equivalent to a thick flat glass in the optical path. However, when thick lead-glass and water medium are added to the optical path of linear structured light measurement, the light will be refracted, which will lead to a large deviation of the measurement results. So, the 3D reconstruction quality and measurement accuracy of the system are reduced. This is a common problem when cameras used in underwater due to the complexity and particularity of the underwater environment [15–17]. In order to improve the measurement accuracy of the underwater vision system, scholars from various countries have done a lot of exploration and research over the years.

LSL sensors are widely used in underwater applications [18–21]. In the early 1990s, Stephen Tetlow and John Spours [22] first proposed the underwater application of the LSL sensor, but they did not address the problem of underwater refraction introducing measurement errors. Xie Zexiao [23] et al. and Albert Palomer [24] et al. established the underwater LSL measurement system using galvanometer, and put forward a calibration method to correct the measurement error caused by refraction.

This paper established a measurement model of linear structured light in underwater environment, and the measurement error caused by the water-glass interface and glass-air interface is corrected based on the model. As shown in Fig. 4, the right-angle reflection prism is equivalent to a thick flat glass in the optical path. The blue-line is the intersection line between the laser plane from the laser and the surface of the object. Point $P(x, y, z)$ in the coordinate system $O_sX_sY_sZ_s$ of the LSL sensor, is the point to be measured on the blue-line. The light reflected by object surface's point P pass through the optical path P N-NM-MOc into the camera

of the LSL sensor. Because the measurement model of the LSL sensor is built and calibrated in the air, the sensor considers that the measurement point is the intersection $P'(x_{gw}, y_{gw}, z_{gw})$ which is the inverse extension line of OcM and the laser plane. That is, the LSL thinks that the point it's measuring comes from the green dotted line.

After calibration of the LSL sensor in air, the camera lens focus $Oc(x_1, y_1, z_1)$ is a given point in the coordinate system $O_sX_sY_sZ_s$ of LSL sensor. The thickness of the lead-glass t value can be measured by calipers. The refractive index of water n_w, the refractive index of lead-glass n_g, and the refractive index of air n_a are known parameters. The distance between coordinate system $O_sX_sY_sZ_s$ and the lead-glass is d, which can be obtained by calibration. The angle between the ray PN and the normal vector of the lead-glass interface is θ_w. The angle between the ray NM and the normal vector of the lead-glass interface is θ_{g1}. The angle between the ray MOc and the normal vector of the lead-glass interface is θ_a. According to Snell's law of refraction:

$$n_w \sin \theta_w = n_g \sin \theta_{g1} = n_g \sin \theta_{g2} = n_a \sin \theta_a \qquad (1)$$

As shown in Fig. 4, in order to analyze the coordinate relationship between $P(x, y, z)$ and $P'(x_{gw}, y_{gw}, z_{gw})$ points, draw a line parallel to line MP' through N points, and intersect the laser plane at point $P''(x_g, y_g, z_g)$. Glass-air interface refraction and water-glass interface refraction only lead to the shift of the measured data in the Z-axis direction. The length of line segment $P'P''$ is the offset caused by glass-air interface, and the length of $P''P$ is the offset caused by water-glass interface. Then, the comprehensive deviation caused by glass-air interface and water-glass interface can be
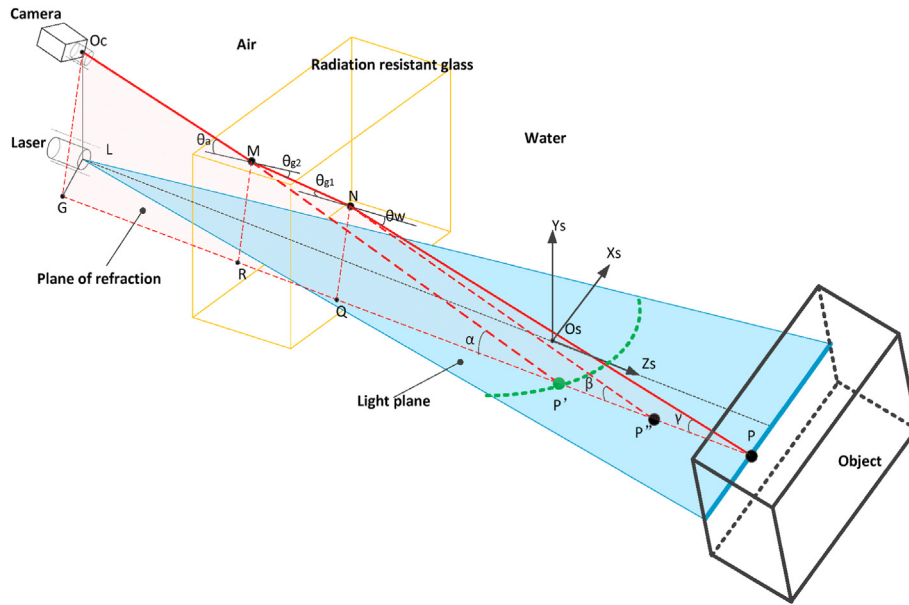
Fig. 4. Model of error caused by flat glass and water.

expressed as the following formula:

$$\delta_{gw} = \delta_g + \delta_w \tag{2}$$

According to the geometric relation, then:

$$\sin \theta_a = \frac{O_C G}{O_C P\prime} = \frac{\sqrt{x_{gw}^2 + y_1^2}}{\sqrt{x_{gw}^2 + y_1^2 + (z_1 - z_{gw})^2}} \tag{3}$$

The offset δ_g between point P′ and point P″ caused by glass-air interface can be expressed as:

$$\delta_g = P\prime P'' = t\left(1 - \frac{\sqrt{1 - \sin^2 \theta_a}}{\sqrt{n_g^2 - \sin^2 \theta_a}}\right) \tag{4}$$

The deviation δ_w between point P and point P″ caused by water-glass interface can be expressed as the following formula:

$$\delta_w = P'' P = PQ - P'' Q \tag{5}$$

$$PQ = \frac{QN}{\tan \theta_w} \tag{6}$$

$$QN = P'' Q * \tan \theta_a \tag{7}$$

$$P\prime Q = |z_Q| + z_{gw} = d + z_{gw} \tag{8}$$

$$P'' Q = P'' P\prime + P\prime Q = \delta_g + d + z_{gw} \tag{9}$$
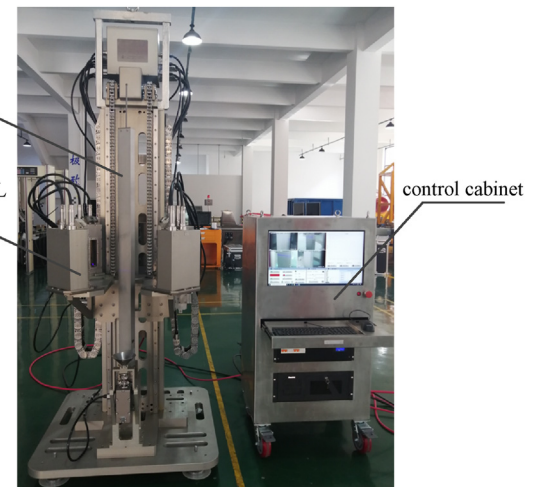
By equations (1)–(9), then:

Fig. 6. The underwater LSL measurement system for spent fuel assemblyIn order to test the performance of the system, a simulated fuel assembly is designed and manufactured and an underwater experiment is carried out. Fig. 7 (a) shows the underwater 3D reconstruction experiment for the underwater LSL measurement system in spent fuel pool, Fig. 7 (b) shows the reconstructed 3D model of the simulated fuel assembly. The size of the simulated fuel assembly is consistent with the size of the real fuel assembly. In this paper, the model is imported into Geomagic wrap 2017 for processing and measurement, and the measurement results are compared with the actual size to verify the reliability of the measurement results.
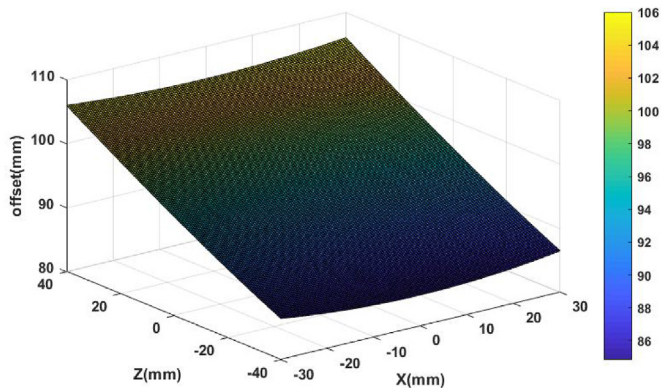

Fig. 5. The offset of measurement value of LSL module with different X and Z coordinates.
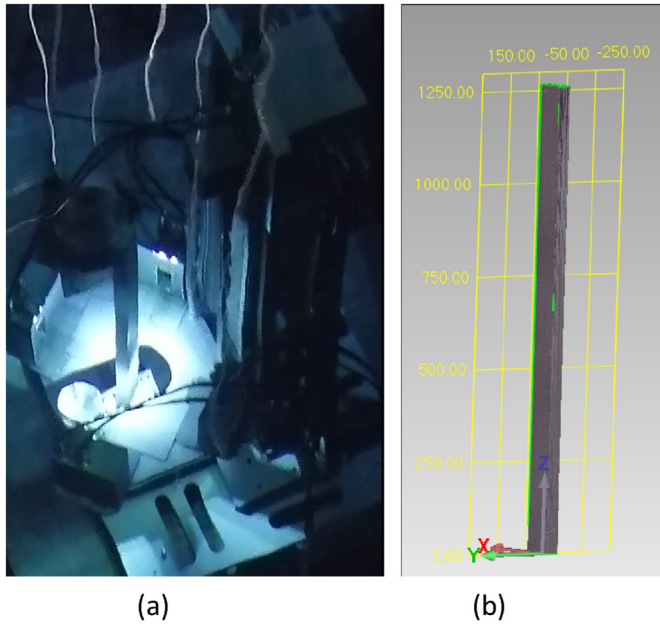
(a)　　　　　　　　　　(b)

Fig. 7. Underwater 3D reconstruction experiment for the underwater LSL measurement system.(a)Underwater experiment; (b) The reconstructed 3D model of the simulated fuel assembly.

$$\delta_w = \frac{(\delta_g + d + z_{gw})\tan\theta_a}{\tan\theta_w} - d - z_{gw} - \delta_g \tag{10}$$

Therefore, the comprehensive offset of the measured data of the underwater LSL measurement module caused by the refraction of the water-glass and glass-air interface can be expressed as:

$$\delta_{gw} = \frac{\left(t\left(1 - \frac{\sqrt{1-\sin^2\theta_a}}{\sqrt{n_g^2 - \sin^2\theta_a}}\right) + d + z_{gw}\right)\sqrt{n_w^2 - \sin^2\theta_a}}{\sqrt{1 - \sin^2\theta_a}} - d - z_{gw} \tag{11}$$

Therefore, the coordinate of the point P to be measured is:

$$x = x_{gw}, y = y_{gw} \tag{12}$$

$$z = z_{gw} + \delta_{gw} = \frac{\left(t\left(1 - \frac{\sqrt{1-\sin^2\theta_a}}{\sqrt{n_g^2 - \sin^2\theta_a}}\right) + d + z_{gw}\right)\sqrt{n_w^2 - \sin^2\theta_a}}{\sqrt{1 - \sin^2\theta_a}} - d \tag{13}$$

According to equation (13), the derivative analysis of relevant parameters can be obtained as follows. The offset of the measured data of the underwater LSL measurement module due to the refraction of the water-glass and glass-air interface is a monotonically increasing function of the flat glass thickness t, and is a monotonically increasing function of the parameter d, and is a monotonically increasing function of the refractive index of boric acid water n_w. In addition, the offset is related to the X-axis co-ordinates of the point P to be measured, when $x_{gw} < 0$, is a monotonically decreasing function of x_{gw}; when $x_{gw} > 0$, is a monotonically increasing function of x_{gw}. Moreover, the offset is related to the Z-axis coordinates of the point P to be measured and increases with the increase of z_{gw}.

In this paper, the equivalent thickness is 60 mm of the lead-glass of the underwater LSL measurement module, and the refractive index of the lead-glass is 1.7, and the refractive index of water is 1.33. The distance between the sensor coordinate system $O_sX_sY_sZ_s$ and the flat lead-glass is 140.00 mm which can be calculated by calibration. The offset of the measured data of the LSL measurement module varies with the X-coordinate value and Z-coordinate value of the measured point, as shown in Fig. 5.

3. Experiment

Fig. 6 shows the underwater LSL measuring system for spent fuel assembly. The total weight is about 650 kg and the overall size is 900mm × 700mm × 2050 mm. In Fig. 6, the left side is the underwater LSL measurement body, and the right side is the control cabinet. Four LSL measuring instruments with LSL sensor (KEYENCE LG-200) are mounted on the upper plane of the lifting platform, so the laser plane can be considered parallel to the upper plane of the lifting platform. The verticality between the upper plane of the lifting platform and the guide rail is ±0.02 mm as measured by Statuspro T430 and R545. The lead screw uses a high-precision ball screw, and the pitch of the lead screw is 5 mm. The upper end of the lead screw is connected with a 5000-line encoder (OMRON E6D-CWZ1E), which can ensure the positional accuracy of the scanning motion. The transformation relationship between the
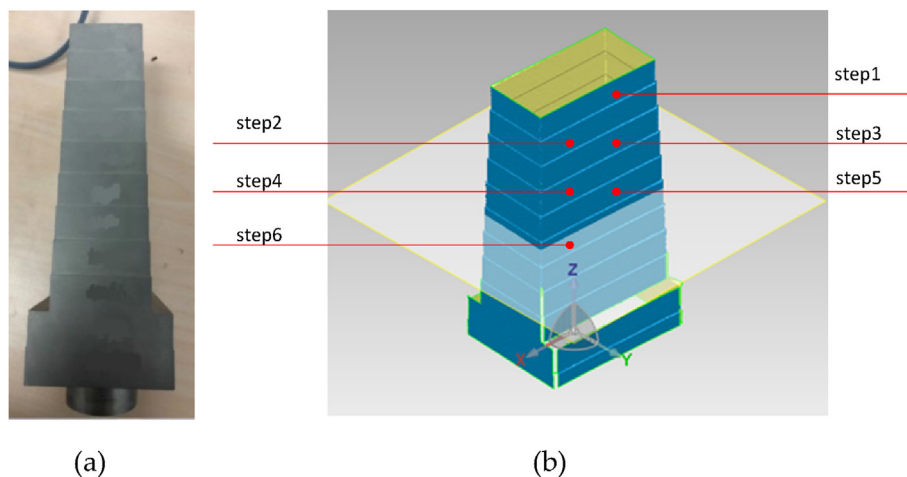

(a)　　　　　　　　　　(b)

Fig. 8. Measurement experiment of standard part.(a) The picture of standard part; (b) The reconstruction model of standard part.

Table 1
The length and width of steps of the standard part, respectively measured by the coordinate measuring machine and the underwater LSL measurement system.

Area to be measured	Dimensions measured by the three-dimensional measuring machine (mm)(The average of the 10 measurements)	Dimensions measured by underwater LSL measurement system (mm)(The average of the 10 measurements)	error value(mm)
The width of Step 1	37.91	37.95	0.04
The length of Step 1	74.92	74.88	−0.04
The width of Step 2	38.93	38.89	−0.04
The length of Step 2	76.91	76.88	−0.03
The width of Step 3	38.90	38.93	0.03
The length of Step 3	78.01	77.99	−0.02
The width of Step 4	39.90	39.90	0
The length of Step 4	79.01	78.97	−0.04
The width of Step 5	41.00	41.05	0.05
The length of Step 5	80.03	80.05	0.02
The width of Step 6	42.01	42.03	0.02
The length of Step 6	81.02	81.04	0.03

coordinate system of each LSL measuring instrument and the world coordinate system was calibrated [7].

To verify the measurement accuracy of the underwater LSL measurement system for spent fuel assembly, the standard part as shown in Fig. 8 (a) is designed and processed. The standard part provides 9 different sizes of steps that are close to the theoretical size of the spent fuel assembly in length and width. The reconstruction model of standard part reconstructed by Geomagic wrap 2017 is shown in Fig. 8(b). Table 1 shows the opposite margin distance of the standard part shown in Fig. 8 (b), respectively measured by the three-dimensional measuring machine (PMM GANTRY202010, with an accuracy of ±(2.2+L/350)μm) and the underwater LSL measurement system. The measurement results show that the measurement error of opposite margin distance of the standard part measured by the measurement system is less than ±0.05 mm.

4. Conclusions

In this paper, a method of non-contact underwater measurement of spent fuel assemblies is proposed. The complete cross-section profile data of fuel assemblies can be collected by multiple linear structured light sensors which can work in radiation environment and underwater environment, and the shape data of the whole spent fuel assembly can be collected by one-dimensional scanning motion. At the same time, the influence of the parameters on the measured data of the linear structured light sensor is analyzed, and the mathematical model of measurement error correction is established. In order to verify the feasibility of the proposed method, a series of underwater measurement experiments were carried out. The system is verified to have the function of 3D reconstruction of spent fuel assemblies by measuring simulated spent fuel assemblies, and the measurement accuracy of the system is verified by measuring standard blocks, and the measurement error is less than ±0.05 mm.

Declaration of competing interest

The authors declared that they have no conflicts of interest to this work.

References

[1] Ahlberg,4-FACE FUEL INSPECTION. https://www.ahlbergcameras.com.System.
[2] A. Sanchez Siguero, A. Sola, Capacity of the equipment family SICOM to inspect fuel elements, in: 39 Annual Meeting of Spanish Nuclear Society, 39. Reunion Anual Sociedad Nuclear Espanola, Reus, Tarragona (Spain), 2013. September 25-27.
[3] S. Sasaki, K. Abe, T. Nagamine, Measurement of deformation of FBR fuel assembly wrapper tube by an innovative technique, in: 2008 KAERI/JAEA Joint Seminar on Advanced Irradiation and PIE Technologies, Daejeon, Korea, 2008. November 5-7.
[4] P.S. Zavyalov, E.S. Senchenko, L.V. Finogenov, et al., A structured-light method for the measurement of deformations in fuel assemblies in the cooling ponds of nuclear power plants, Russ. J. Nondestr. Test. 48 (2012) 705–711.
[5] J. Cho, Y. Choi, K. Jeong, et al., Measurement of nuclear fuel rod deformation using an image process technique, Nucl. Eng. Technol. 43 (2011) 133–140.
[6] C. Wang, H.U. Song, C. Feng, et al., Deformation detection system of fuel assembly based on underwater binocular vision, J. Appl. Opt. 40 (2019) 58–63.
[7] J. Zhao, C. Feng, G. Cai, R. Zhang, et al., Three-dimensional reconstruction and measurement of fuel assemblies for sodium-cooled fast reactor using linear structured light, Ann. Nucl. Energy 160 (2021), 108397.
[8] R.E. Sharp, D.R. Garlick, Radiation Effects on Electronic Equipment, a Designers'/users' Guide for the Nuclear Power Industry, 1994. United Kingdom.
[9] J.R. Srour, J.W. Palko, Displacement damage effects in irradiated semiconductor devices, IEEE Trans. Nucl. Sci. 60 (2013) 1740–1766.
[10] J.R. Srour, J.W. Palko, A framework for understanding displacement damage mechanisms in irradiated silicon devices, IEEE Trans. Nucl. Sci. 53 (2006) 3610–3620.
[11] J. Bogaerts, B. Dierickx, R. Mertens, Enhanced dark current generation in proton-irradiated CMOS active pixel sensors, IEEE Trans. Nucl. Sci. 49 (2002) 1513–1521.
[12] V. Goiffon, M. Estribeau, O. Marcelot, et al., Radiation effects in pinned photodiode CMOS image sensors: pixel performance degradation due to total ionizing dose, IEEE Trans. Nucl. Sci. 59 (2012) 2878–2887.
[13] B. Speit, E. Rädlein, G.H. Frischat, et al., Radiation resistant optical glasses, Nucl. Instrum. Methods Phys. Res. B. 65 (1992) 384–386.
[14] W. Li, M. Lu, The effect of added O2 on the transmittance and radiation resistance of radiation resistant glasses, Opt Express 18 (2010) 26307–26312.
[15] A. Palomer, P. Ridao, J. Forest, et al., Underwater laser scanner: ray-based model and calibration, IEEE ASME Trans. Mechatron. 24 (2019) 1986–1997.
[16] A. Agrawal, S. Ramalingam, Y. Taguchi, et al., A theory of multi-layer flat

refractive geometry, in: 2012 IEEE Conference on Computer Vision and Pattern Recognition, IEEE, RI, USA, 2012. June 16-21.

[17] T. Treibitz, Y. Schechner, C. Kunz, et al., Flat refractive geometry, IEEE Trans. Pattern. Anal. 34 (2012) 51—65.

[18] C.C. Wang, D. Tang, Seafloor roughness measured by a laser line scanner and a conductivity probe, IEEE J. Ocean. Eng. 34 (2009) 459—465.

[19] H.R. Cui, C.F. Guo, S.L. Lan, 3D Reconstruction for Underwater Target Based on Linear Structured Light, 2014 Applied Mechanics and Materials, Switzerland, 2014, pp. 660—664.

[20] S.G. Narasimhan, S.K. Nayar, Structured light methods for underwater imaging: light stripe scanning and photometric stereo, in: Proceedings of OCEANS 2005, MTS/IEEE, Washington, USA, 2005. September 17-23.

[21] P. Risholm, T. Kirkhus, J.T. Thielemann, et al., Adaptive structured light with scatter correction for high-precision underwater 3D measurements, Sensors 19 (2019), 19051043.

[22] S. Tetlow, J. Spours, Three-dimensional measurement of underwater work sites using structured laser light, Meas. Sci. Technol. 10 (1999) 1162—1167.

[23] S. Chi, Z. Xie, W. Chen, A laser line auto-scanning system for underwater 3D reconstruction, Sensors 16 (2016), 16091534.

[24] A. Palomer, P. Ridao, D. Youakim, et al., 3D laser scanner for underwater manipulation, Sensors 18 (2018), 18041086.